Human Cancer Biology

IFITM1 promotes the invasion at the early stage of head and neck cancer progression

Hiroko Hatano[1], Yasusei Kudo[1, *], Ikuko Ogawa [2], Akira Kikuchi[3], Yoshimitsu Abiko[4], Takashi Takata[1, *]

[1]Department of Oral and Maxillofacial Pathobiology, Division of Frontier Medical Science, Graduate School of Biomedical Sciences, Hiroshima University, [2]Center of Oral Clinical Examination, Hiroshima University Hospital, Hiroshima University, [3]Department of Biochemistry, Graduate School of Biomedical Sciences, Hiroshima University, Hiroshima 734-8553, Japan, [4]Department of Biochemistry, School of Dentistry at Matsudo, Nihon University, 270-8587, Japan.

Running title: IFITM1 promotes invasion of HNSCC cells

***Correspondence to:** Department of Oral and Maxillofacial Pathobiology, Division of Frontier Medical Science, Graduate School of Biomedical Sciences, Hiroshima University, 1-2-3 Kasumi, Minami-ku, Hiroshima 734-8553, Japan. Fax: +81-82-257-5619, E-mail: ykudo@hiroshima-u.ac.jp and ttakata@hiroshima-u.ac.jp

Abstract

Purpose: Head and neck squamous cell carcinoma (HNSCC), one of the most common types of human cancer, show persistent invasion that frequently leads to local recurrence and distant lymphatic metastasis. However, molecular mechanisms associated with invasion of HNSCC remain poorly understood. We identified Interferon-induced transmembrane protein 1 (IFITM1) as a candidate gene for promoting the invasion of HNSCC by comparing the gene expression profiles between parent and a highly invasive clone. Therefore, we examined the role of IFITM1 in the invasion of HNSCC.

Experimental Design: IFITM1 expression was examined in HNSCC cell lines and cases by RT-PCR and immunohistochemistry. IFITM1 overexpressing and knockdown cells were generated, and the invasiveness of these cells was examined by *in vitro* invasion assay. Gene expression profiling of HNSCC cells overexpressing IFITM1 versus control cells was examined by microarray.

Results: HNSCC cells expressed IFITM1 mRNA at higher levels, while normal cells did not express. By immunohistochemistry, IFITM1 expression was observed in early invasive HNSCC and invasive HNSCC. Interestingly, IFITM1 was expressed at the invasive front of early invasive HNSCC, and higher expression of IFITM1 was found in invasive HNSCC. In fact, IFITM1 overexpression promoted and IFITM1 knockdown suppressed the invasion of HNSCC cells *in vitro*. Gene expression profiling of HNSCC cells overexpressing IFITM1 versus control cells revealed that several genes including matrix metalloproteinase were up-regulated in IFITM1 overexpressing cells.

Conclusion: Our findings suggest that IFITM1 plays an important role for the invasion at the early stage of HNSCC progression, and that IFITM1 can be a therapeutic target for HNSCC.

Key Words: IFITM1, invasion, head and neck cancer

Abbreviations: HNSCC: head and neck squamous cell carcinoma; IFITM1: Interferon-induced transmembrane protein 1; MMP: matrix metalloproteinase; RT-PCR: Reverse-Transcription polymerase chain reaction; PBS: phosphate-buffered saline.

Introduction

Head and neck squamous cell carcinoma (HNSCC) is one of the most common types of human cancer, with an annual incidence of more than 500,000 cases worldwide (1). The extent of lymph node metastasis is a major determinant in the prognosis of HNSCC. Like most epithelial cancers, HNSCC develops through the accumulation of multiple genetic and epigenetic alterations in a multi-step process (2). Recent molecular studies have advanced our understanding of the disease and provided a rationale to develop novel strategies for early detection, classification, prevention and treatment. Attempts to identify the genes involved in the metastasis are pivotal for the early prediction of HNSCC behavior. The process of metastasis consists of sequential and selective steps including proliferation, induction of angiogenesis, detachment, motility, invasion into circulation, aggregation and survival in the circulation, cell arrest in distant capillary beds and extravasation into organ parenchyma (2). We previously established an HNSCC cell line, MSCC-1, from lymph node metastasis (3). Moreover, we isolated a highly invasive clone MSCC-Inv1 from MSCC-1 cells by using an *in vitro* invasion assay device (4). Then, we compared the transcriptional profile of parent cells (MSCC-1) and a highly invasive clone (MSCC-Inv1) by microarray analysis in order to identify genes that differ in their expression (5). Several genes were selectively overexpressed in the highly invasive clone. Among these genes, the most highly expressed gene was Periostin, and the second was IFITM1. In fact, we demonstrated that Periostin promoted invasion both *in vitro* and *in vivo* (5).

IFITM1, also known as 9-27 or Leu13, is a member of the interferon-inducible transmembrane protein family. *IFITM1* gene product was initially identified as Leu13, a leukocyte antigen that is a part of a membrane complex involved in the transduction of antiproliferative and homotypic adhesion signals in lymphocytes (6-9). Moreover, IFITM1 is a 17-kD membrane protein that was inducible on tumor cell lines by interferon-alpha and

usually to a lesser extent, by interferon (10). However, there have been a few papers of IFITM1 in cancer and the role of IFITM1 in cancer is poorly understood. In the present study, therefore, we examined the roles of IFITM1 for HNSCC invasion.

Materials and methods

Cell culture

MSCC-1 and MSCC-Inv1 cells were previously established in our laboratory (Kudo et al., 2003; Kudo et al., 2004). These cells were maintained in Keratinocyte-SFM (Invitrogen) under a condition of 5 % CO_2 in air at 37 ˚C. HNSCC cell lines (HSC2, HSC3, HSC4, Ca9-22, Ho-1-N-1 and Ho-1-U-1) were provided by Japanese Collection of Research Bioresources Cell Bank. They were maintained in RPMI-1640 (Nissui Pharmaceutical Co., Tokyo, Japan) supplemented with 10 % heat-inactivated FBS (Invitrogen) and 100 U/ml penicillin-streptomycin (Gibco) under conditions of 5 % CO_2 in air at 37 ˚C. Normal oral epithelial cells and gingival fibroblasts were obtained from oral mucosa or gingival tissues using standard explant techniques (11). These tissues were obtained from routine dental surgery in the Department of Oral Surgery, Hiroshima University Hospital. Normal oral epithelial cells were routinely maintained in Keratinocyte-SFM (GIBCO BRL, Grand Island, NY) and gingival fibroblasts were maintained in Dulbecco's modified Eagle's medium (DMEM) supplement with 10 % fetal bovine serum. For growth assay, cells were plated on 24 well plates (Falcon), and trypsinized cells counted by Cell Counter (Coulter Z1).

RT-PCR

Total RNA was isolated from cultures of confluent cells using the RNeasy Mini Kit (Qiagen). Preparations were quantified and their purity was determined by standard spectrophometric methods. cDNA was synthesized from 1 □μg total RNA according to

the ReverTra Dash (Toyobo Biochemicals, Tokyo, Japan). Primer sequences were listed in Table 1A. Aliquots of total cDNA were amplified with Go Taq® Green Master Mix (Promega), and amplifications were performed in a PC701 thermal cycler (Astec, Fukuoka, Japan) for 25 (IFITM1 and CD81) or 30 (GAPDH, ßTrcp-1, ßTrcp2, ZNF236, MMP13 and MMP12) cycles after an initial 30 sec denaturation at 94 ˚C, annealed for 30 sec at 60 ˚C, and extended for 1 min at 72 ˚C in all primers. The amplification reaction products were resolved on 1.5% agarose/TAE gels (Nacalai tesque, Inc., Kyoto, Japan), electrophoresed at 100 mV, and visualized by ethidium-bromide staining.

Western blot analysis

Western blotting was carried out as we described previously (5). An anti-IFITM1 polyclonal antibody (Boster Biological Technology. Ltd, Wuhan, China), anti-FLAG monoclonal antibody (Sigma) and anti-Cul1 polyclonal antibody (Zymed) were used. Thirty μg of protein was subjected to 10 % polyacrylamide gel electrophoresis followed by electroblotting onto a nitrocellulose filter. For detection of the immunocomplex, the ECL western blotting detection system (Amersham) was used.

Tissue samples

Tissue samples of HNSCC were retrieved from the Surgical Pathology Registry of Hiroshima University Hospital, after approval by the Ethical Committee of our institutions. Twenty cases of frankly invasive HNSCC, 11 early invasive HNSCC and 10 normal oral mucosal tissues were used in this study. 10 % buffered-formalin fixed and paraffin embedded tissues were used for immunohistochemical examination. The histological grade and stage of tumor were classified according to the criteria of the Japan Society for Head and Neck Cancer.

Immunohistochemical staining

Immunohistochemical detection of IFITM1 in HNSCC cases was performed on 4.5 μm sections mounted on silicon-coated glass slides, using a streptavidin-biotin peroxidase technique as described previously (12).

Generation of IFITM1-overexpressing HNSCC cells

Human *IFITM1* cDNA was isolated from the cDNA by RT–PCR using sense and antisense primers. Human *IFITM1* cDNA was then subcloned by insertion into the *Eco*RI/*Bam*HI restriction site of pBICEP-CMV-2 (Sigma). The IFITM1-pBICEP-CMV-2 plasmid or the vector alone was introduced into Ca9-22 cells, and the stable clones were obtained by G418 selection (500 μg/ml, Gibco) in the culture medium. We obtained pool and 4 stable clones. Cell transfection was performed using FuGENE 6 HD (Roche) according to the manufacture's instruction.

***In vitro* invasion assay**

In vitro invasion assay was performed as described previously (4,13). Briefly, invasion was measured by use of a 24 well cell culture insert with 8 μm pores (3097, Falcon, Becton Dickinson, Franklin Lakes, NJ). The filter was coated with 50 μg of Matrigel (Becton Dickinson), which was reconstituted basement membrane substance. The lower compartment contained 0.5 ml of serum-free medium. After trypsinization, 1.5 x 10^5 cells were resuspended in 100 μl of serum-free medium and placed in the upper compartment of the cell culture insert for 24 hours. To examine the invasiveness, penetrated cells onto the lower side of the filter were fixed with formalin and stained with hematoxylin. We assayed 3 times.

Wound healing assay

For the wounding healing experiment, cells were seeded on 6 well plates and cells were allowed to grow to complete confluence. Subsequently, a plastic pipette tip was used to scratch the cell monolayer to create a cleared area, and the wounded cell layer was washed with fresh medium to remove loose cells. Immediately following scratch wounding (0 h) and after incubation of cells at 37 °C for 24 h, phase-contrast images (10x field) of the wound healing process were photographed digitally with an inverted microscope. The distance of the wound areas were measured on the images, set at 100% for 0 h, and the mean percentage of the total distances of the wound areas was calculated.

RNA interference experiments

shRNAs were designed based on the prediction of publicly available prediction programs (14), which are summarized in Table 1B. shRNAs were cloned into the transient micro-RNA expression vector pcDNA6.2-GW/emGFP/miR (Invitrogen), which co-expresses the shRNA surrounded by miR-155–flanking sequences together with emGFP. Logarithmically growing Ca9-22 and HSC2 cells were seeded at a density of 10^5cells/6cm dish and were transfected. After 48h of transfection, we treated blasticidin for 10 days. After selection, we obtained the stably shRNA expressing cells. si-miR-neg, provided by Invitrogen, has an insert that can form a hairpin structure that is processed into mature miRNA, but it is predicted not to target any known vertebrate gene (according to Invitrogen). Transfection efficiency was checked by GFP expression under UV microscopy and by RT-PCR.

For knockdown of ß-Trcp, we used the siRNA oligos. The siRNA oligos used for both ß-Trcp1 and ß-Trcp2 silencing were 21 bp synthetic molecules (Dharmacon Research) corresponding to nt 407-427 of human ß-Trcp1 and 161-181 of human ß-Trcp2 (AB033279)

(15). A 21 nt siRNA duplex corresponding to a non-relevant F-Box protein (Fbp) gene was used as a control. Logarithmically growing Ca9-22 cells were seeded at a density of 10^5cells/6cm dish and transfected with oligos twice (at 24 and 48 hr after replating) using Oligofectamine (Invitrogen) as described (16). Forty-eight hours after the last transfection, lysates were prepared and analyzed by SDS-PAGE and immunobloting.

Gene array analysis

The human focus array using the system containing 50000 genes probes was used for comparing the transcriptional profiles between IFITM1 overexpressing Ca9-22 cells and control Ca9-22 cells. This array contains a broad range of genes derived from publicly available, well-annotated mRNA sequences. Total RNA was isolated from cultures of confluent cells using the RNeasy Mini Kit (Qiagen) according to the manufacturer's instructions. Preparations were quantified and their purity was determined by standard spectrophometric methods. Data were expressed as the average differences between the perfect match and mismatch probes for the IFITM1 gene.

Results

IFITM1 overexpression is frequently found in HNSCC.

We previously identified IFITM1 as an invasion-promoting factor of HNSCC by comparing the transcriptional profile of parent HNSCC cells (MSCC-1) and a highly invasive clone (MSCC-Inv1) (5). The finding of higher expression of IFITM1 in the highly invasive clone than the parent cells was confirmed by RT-PCR (Fig. 1A). Next, we examined the IFITM1 mRNA in 6 HNSCC cell lines, normal oral epithelial cells and normal gingival fibroblasts. IFITM1 mRNA expression was observed in all HNSCC cell lines, but not in normal

epithelial cells and fibroblasts (Fig. 1B). IFITM1 protein expression was examined by Western blot analysis in HNSCC cells, and anti-IFITM1 antibody recognized IFITM1 protein (Fig. 1C). By using this antibody, we examined the expression of IFITM1 by immunohistochemistry to know the localization of IFITM1 in HNSCC. Twenty cases of frankly invasive HNSCC, 11 early invasive HNSCC and 10 normal oral mucosal tissues were used in this study. In normal oral epithelium, only basal cells slightly expressed IFITM1 in their cytoplasm and membrane (Fig. 1D). In early invasive HNSCC, surrounding cells in cancer nests of invasive front expressed IFITM1 at higher levels in comparison with basal cells in normal epithelium (Fig. 1D). In frankly invasive HNSCC, cancer cells expressed IFITM1 at higher levels in their cytoplasm and membrane (Fig. 1D). As all cancer cases expressed IFITM1 at higher levels, we could not compare with clinico-pathological findings including histological differentiation and metastasis. Thus, high expression of IFITM1 was focally observed in invasive front of early invasive HNSCC and diffusely observed in invasive HNSCC. This finding suggests that IFITM1 may be involved in the invasion at the early stage of HNSCC progression. For further evaluation of IFITM1 expression in patients with HNSCC, we compared the expression in a previously published microarray dataset of 41 HNSCC patients and 13 normal controls (17). Similar to our data, IFITM1 was expressed at higher levels in HNSCC tissues, in comparison with normal oral mucosal tissues (Fig. 1E).

IFITM1 is involved in the invasion of HNSCC cells.

To demonstrate the involvement of IFITM1 in the invasion of HNSCC, we generated the IFITM1 overexpressing cells. We transfected IFITM1 into Ca9-22 cells that showed low expression of IFITM1. Then, we obtained 3 stable clones of IFITM1 expressing cells (Fig. 2A). IFITM1 overexpression did not change the cell proliferation (Fig. 2B). We

compared the invasiveness between control and IFITM1 overexpressing HNSCC cells. By *in vitro* invasion assay, IFITM1 overexpression enhanced the invasion (Fig. 2C). Moreover, IFITM1 overexpression enhanced the migration by wound healing assay (Fig. 2D). To confirm the IFITM1-mediated invasion of HNSCC cells, we examined the knockdown of IFITM1 by using short hairpin RNAs (shRNAs) in HSC2 cells with high expression of IFITM1. We designed three different short hairpin RNAs (#1, #2 and #3) and transfected them into HSC2 cells. All shRNAs reduced the IFITM1 expression (Fig. 3A). IFITM1 shRNAs did not influence the cell proliferation (Fig. 3B), but IFITM1 shRNAs remarkably inhibited the invasion of HNSCC cells (Fig. 3C).

CD81 is involved in the invasion of HNSCC cells

CD81 is a widely expressed cell-surface protein involved in an astonishing variety of biologic responses (18). CD81 associates on the surface of B cells in a molecular complex that includes the B-cell-specific molecules CD19 and CD21 and Leu-13/IFITM1 (18). As we thought that CD81 may be involved in IFITM1 mediated invasion of HNSCC cells, we examined the correlation between CD81 and IFITM1 expression in HNSCC cells. First, we examined the expression of CD81 mRNA in HNSCC cell lines and normal cells. In similar to IFITM1 expression, CD81 expression was observed only in HNSCC cells, but not in normal oral epithelial cells and gingival fibroblasts (Fig. 4A). To check the correlation between IFITM1 and CD81, we examined the CD81 expression in IFITM1 overexpressing and IFITM1 knockdown cells. Although IFITM1 overexpression enhanced CD81 expression, IFITM1 knockdown did not affect CD81 expression (Fig. 4B). To know the role of CD81 for the invasion of HNSCC cells, we examined the knockdown of CD81 in HSC2 cells by using shRNA. We designed three different short hairpin RNAs (#1, #2 and #3) and transfected them into HSC2 cells. All shRNAs reduced CD81

expression, but did not influence on IFITM1 expression (Fig. 5A). In similar to the phenotype of IFITM1 knockdown cells, CD81 knockdown remarkably inhibited the invasion of HNSCC cells (Fig. 5B). Moreover, we transfected three different CD81 shRNA into the IFITM1 overexpressing HNSCC cells (Fig. 5C). CD81 knockdown inhibited the IFITM1 enhanced invasion of HNSCC cells, indicating that CD81 may be involved in the invasion of HNSCC cells (Fig. 5C).

Recent studies have shown that during embryogenesis, BMP4 and Wnt/ß-catenin signaling were able to control the level of expression of IFITM1, and that IFITM1 is induced by activation of the Wnt/ß-catenin signaling during intestinal tumorigenesis (19,20). Therefore, we examined whether overexpression of IFITM1 in HNSCC cells is induced by activation of the Wnt/ß-catenin signaling. ß-Trcp siRNA treatment induced ß-catenin accumulation, indicating the activation of the Wnt/ß-catenin signaling (Fig. 5D). However, IFITM1 was not up-regulated in ß-Trcp siRNA treated HNSCC cells (Fig. 5D).

IFITM1 overexpression induces up-regulation of MMP.

To know the mechanism of IFITM1 for the invasion of HNSCC cells, we compared the gene transcriptional profiles of control and IFITM1 overexpressing HNSCC cells. By microarray analysis, several genes were selectively overexpressed in IFITM1 overexpressing HNSCC cells (Table 2). Among these genes, ZNF236 was the most highly expressed gene. ZNF236, a novel Kruppel-like zinc-finger gene was initially identified by its glucose-regulated expression in human mesangial cells using mRNA differential display (21). In addition, MMP13 and MMP12 were up-regulated in IFITM1 overexpressing HNSCC cells. Certain aspects of MMP involvement in tumor metastasis such as tumor-induced angiogenesis, tumor invasion, and establishment of metastatic foci at the secondary site, have received extensive attention that resulted in an overwhelming

amount of experimental and observational data in favor of critical roles of MMPs in these processes (22). Highly expression of ZNF236, MMP13 and MMP12 in IFITM1 overexpressing HNSCC cells was confirmed by RT-PCR (Fig. 5E).

Discussion

We previously identified several genes, which encode secretary or cell surface proteins implicated in invasion, cell adhesion, angiogenesis and growth factor as a candidate gene for the invasion of HNSCC by comparing the gene expression profiles between parent HNSCC cells and a highly invasive clone using microarray analysis (5). IFITM1 was the second of overexpressed genes in highly invasive clones and we considered as a novel candidate gene for HNSCC invasion. As we expected, IFITM1 overexpression promoted the invasion and migration of HNSCC cells *in vitro* (Fig. 2). These findings are consistent with the recent report that IFITM1 modulates the invasiveness of gastric cancer cells (23). We also found that high expression of IFITM1 was focally observed in invasive front of early invasive HNSCC and diffusely observed in invasive HNSCC by immunohistochemical analysis, suggesting that IFITM1 may be involved in the invasion at the early stage of HNSCC progression. This observation is consistent with recent report that expression of several members of the IFITM family was up-regulated in early and late intestinal neoplasms by using different mouse models of Apc inactivation and human colon tumor samples, and that up-regulation of the *IFITM* genes seems to be an early event in ß-catenin intestinal tumorigenesis (20). We suggest that IFITM1 may be involved in the initial step of invasion such as the degradation of the basement membrane and the interstitial extracellular matrix, which results in cellular infiltration into the adjacent tissue. In our microarray analysis, we identified Periostin as the most highly expressed gene in highly invasive clones (5). In fact, we demonstrated that Periostin dramatically enhanced

invasion, anchorage independent growth both *in vitro* and *in vivo*, and that Periostin overexpression was well correlated with poorly differentiation and metastasis in HNSCC cases by immunohistochemistry (5). We suggested that Periostin overexpression might be a late event such as the aggressive invasion into surrounding tissues, invasion into circulation, and extravasation into organ parenchyma in HNSCC progression. Overall IFITM1 and Periostin can be a marker for predicting the invasion of HNSCC at the early and late stage of HNSCC progression, respectively.

To know the mechanism of IFITM1 for invasion of HNSCC cells, we compared the gene expression profiles between control and IFITM1 overexpressing HNSCC cells. IFITM1 overexpression enhanced MMP12 and MMP13 expression in HNSCC cells (Fig. 5E and Table 1), suggesting that IFITM1 enhanced invasion of HNSCC cells through the activation of certain type of MMP. Previous studies demonstrated that IFITM1 associates with CD81 and make a complex with CD19 and CD21 (18). In addition, it has been reported that constitutive up-regulation of CD81 is associated with an increased growth rate and tumor progression in a mouse model of skin tumor (24). Therefore, we asked whether CD81 was involved in the IFITM1 induced invasion of HNSCC cells or not. In similar to IFITM1 expression, CD81 expression was observed in HNSCC cells, but not in normal cells (Fig. 4A). Interestingly, IFITM1 overexpression enhanced CD81 expression (Fig. 4B) and knockdown of CD81 inhibited the invasion of HNSCC cells in similar to IFITM1 knockdown (Fig. 5B). Moreover, CD81 knockdown abolished IFITM1 induced invasion of HNSCC cells (Fig. 5C). Although these findings suggest that CD81 may be involved in the invasion of HNSCC, the association between IFITM1 and CD81 for the invasion of HNSCC cells is still unclear. As CD81 is associated with integrins (α6ß1 and α3ß1) in HeLa cells (25), CD81 induced invasion may be associate with certain type of integrins. It is also known that CD81 is considered a putative receptor for hepatitis C

virus (26). Therefore, this finding raises the possibility that unknown ligand may bind to CD81 and may be involved in CD81 induced invasion. To demonstrate the detailed molecular mechanisms of IFITM1 and CD81 for cancer invasion, further studies will be required.

In the present study, highly expression of IFITM1 was observed in all HNSCC cancer cell lines and invasive HNSCC cancer cases. Up-regulation of IFITM1 was observed in colon, rectal, stomach and lung cancers by large-scale analysis of IFITM expression (22). Therefore, up-regulation of IFITM1 may be a common event in the progression of various cancers. Recent studies have shown that during embryogenesis, BMP4 and Wnt/ß-catenin signaling were able to control the level of expression of IFITM1, and that IFITM1 is induced after activation of the Wnt/ß-catenin signaling during intestinal tumorigenesis (19,20). However, IFITM1 was not up-regulated by activation of the Wnt/ß-catenin signaling in HNSCC cells (Fig. 5D). To clarify the mechanism of up-regulation of IFITM1 will required further studies. In conclusion, our studies have revealed a critical role of IFITM1 for the invasion at the early stage of HNSCC progression. These findings provide new and important information on the progression of HNSCC and suggest that IFITM1 could be used as a novel molecular target for therapy of HNSCC patients.

Acknowledgements

We thank Dr. P. M. Gaffney for providing us the Gene Chips data of 41 primary HNSCC and 13 normal tissues and Ms. A. Imaoka for supporting microarray analysis. We also thank Dr Kawai and Dr. Kitajima for helpful discussion. Supported by in part by grants-in-aid from the Ministry of Education, Science and Culture of Japan to YK and TT, and grants from Haraguchi cancer memorial foundation to YK.

References

1. Mao L, Hong WK, Papadimitrakopoulou VA. Focus on head and neck cancer. Cancer Cell 2004;5:311-6.
2. Fidler IJ. Critical factors in the biology of human cancer metastasis: Twenty-eighth GHA Clowes Memorial Award Lecture. Cancer Res 1990;50:6130-8.
3. Kudo Y, Kitajima S, Sato S, Ogawa I, Miyauchi M, Takata T. Establishment of an oral squamous cell carcinoma cell line with high invasive and p27 degradation activity from lymph node metastasis. Oral Oncol 2003;39:515-20.
4. Kudo Y, Kitajima S, Ogawa I, Hiraoka M, Salgolzaei S, Keikhaee MR, Sato S, Miyauchi M, Takata T. Invasion and metastasis of oral cancer cells require methylation of E-cadherin and/or degradation of membranous ß-catenin. Clin Cancer Res 2004;10:5455-63.
5. Kudo Y, Ogawa I, Kitajima S, Kitagawa M, Kawai H, Gaffney PM, Miyauchi M, Takata T. Periostin promotes invasion and anchorage-independent growth in the metastatic process of head and neck cancer. Cancer Res 2006;66:6928-35.
6. Chen YX, Welte K, Gebhard DH, Evans RL. Induction of T cell aggregation by antibody to a 16kd human leukocyte surface antigen. J Immunol 1984;133:2496-501.

7. Takahashi S, Doss C, Levy S, Levy R. TAPA-1, the target of an antiproliferative antibody, is associated on the cell surface with the Leu-13 antigen. J Immunol 1990;145:2207-13.
8. Bradbury LE, Kansas GS, Levy S, Evans RL, Tedder TF. The CD19/CD21 signal transducing complex of human B lymphocytes includes the target of antiproliferative antibody-1 and Leu-13 molecules. J Immunol 1992;149:2841-50.
9. Matsumoto AK, Martin DR, Carter RH, Klickstein LB, Ahearn JM, Fearon DT. Functional dissection of the CD21/CD19/TAPA-1/Leu-13 complex of B lymphocytes. J Exp Med 1993;178:1407-17.
10. Deblandre GA, Marinx OP, Evans SS, Majjaj S, Leo O, Caput D, Huez GA, Wathelet MG. Expression cloning of an interferon-inducible 17-kDa membrane protein implicated in the control of cell growth. J Biol Chem 1995;270:23860-6.
11. Schor SL, Schor AM, Rushton G, Smith LJ. Adult, foetal and transformed fibroblasts display different migratory phenotypes on collagen gels: evidence for an isoformic transition during foetal development. Cell Sci 1985;73,221-34.
12. Kitajima S, Kudo Y, Ogawa I, Bashir T, Kitagawa M, Miyauchi M, Pagano M, Takata T. Role of Cks1 overexpression in oral squamous cell carcinomas: cooperation with Skp2 in promoting p27 degradation. Am J Pathol 2004;165:2147-55.
13. Kalebic T, Williams JE, Talmadge JE, Kao-Shan CS, Kravitz B, Locklear K, Siegal GP, Liotta LA, Sobel ME, Steeg PS. A novel method for selection of invasive tumor cells: derivation and characaterization of highly metastatic K1735 melanoma cells based on in vitro and in vivo invasive capacity. Clin Exp Metastasis 1998;6:301-18.
14. Yuan, B., R. Latek, M. Hossbach, T. Tuschl, and F. Lewitter. siRNA Selection Server: an automated siRNA oligonucleotide prediction server. Nucleic Acids Res 2004;32:W130-4.

15. Guardavaccaro D, Kudo Y, Boulaire J, Barchi M, Busino L, Donzelli M, Margottin-Goguet F, Jackson PK, Yamasaki L, Pagano M. Control of meiotic and mitotic progression by the F-box protein ß-Trcp1 in vivo. Dev Cell 2003;4:799-812.

16. Elbashir SM, Harborth J, Lendeckel W, Yalcin A, Weber K, Tuschl T. Duplexes of 21-nucleotide RNAs mediate RNA interference in cultured mammalian cells. Nature 2001;411:494-8.

17. Ginos MA, Page GP, Michalowicz BS, Patel KJ, Volker SE, Pambuccian SE, Ondrey FG, Adams GL, Gaffney PM. Identification of a Gene Expression Signature Associated with Recurrent Disease in Squamous Cell Carcinoma of the Head and Neck. Cancer Res 2004;64:55-63.

18. Levy S, Todd SC, Maecker HT. CD81 (TAPA-1): A molecule involved in signal transduction and cell adhesion in the immune system. Annu Rev Immunol 1998;16:89-109.

19. Lickert H, Cox B, Wehrle C, Taketo MM, Kemler R, Rossant J. Dissecting Wnt/ß-catenin signaling during gastrulation using RNA interference in mouse embryos. Development 2005;132:2599–609.

20. Andreu P, Colnot S, Godard C, Laurent-Puig P, Lamarque D, Kahn A, Perret C, Romagnolo B. Identification of the IFITM family as a new molecular marker in human colorectal tumors. Cancer Res 2006;66:1949-55.

21. Holmes DI, Wahab NA, Mason RM. Cloning and characterization of ZNF236, a glucose-regulated Kruppel-like zinc-finger gene mapping to human chromosome 18q22-q23. Genomics 1999;60:105-9.

22. Deryugina EI, Quigley JP. Matrix metalloproteinases and tumor metastasis. Cancer Metastasis Rev 2006;25:9-34.

23. Yang Y, Lee JH, Kim KY, Song HK, Kim JK, Yoon SR, Cho D, Song KS, Lee YH, Choi I. The interferon-inducible 9-27 gene modulates the susceptibility to natural killer cells and the invasiveness of gastric cancer cells. Cancer Lett 2005;221:191-200.

24. Owens DM, Watt FM. Influence of beta1 integrins on epidermal squamous cell carcinoma formation in a transgenic mouse model: alpha3beta1, but not alpha2beta1, suppresses malignant conversion. Cancer Res 2001;61: 5248-54.

25. Berditchevski F, Zutter MM, Hemler ME. Characterization of novel complexes on the cell surface between integrins and proteins with 4 transmembrane domains (TM4 proteins). Mol Biol Cell 1996;7:193-207.

26. Silvie O, Rubinstein E, Franetich JF, Prenant M, Belnoue E, Renia L, Hannoun L, Eling W, Levy S, Boucheix C, Mazier D. Hepatocyte CD81 is required for Plasmodium falciparum and Plasmodium yoelii sporozoite infectivity. Nat Med 2003;9:93-6.

Figure legends

Fig. 1. Overexpression of IFITM1 in HNSCC. (**A**) Confirmation of higher expression of IFITM1 mRNA in the highly invasive clone by RT-PCR. (**B**) Expression of IFITM1 mRNA in 6 HNSCC cell lines, normal oral epithelial cells and gingival fibroblasts. Expression of IFITM1 mRNA was performed by RT-PCR. (**C**) Expression of IFITM1 protein in 6 HNSCC cell lines by Western blot analysis. Cul1 expression was used as a loading control. (**D**) Expression of IFITM1 was examined by immunohistochemistry in normal oral mucosae (Normal, x40), early invasive HNSCC (early invasive SCC, x40) and invasive HNSCC (SCC, x40). Representative cases of IFITM1 expression were shown. (**E**) Total RNA from 41 primary HNSCC and 13 normal tissues was labeled and hybridized to Affymetrix U133A Gene Chips as previously reported (17). Graph shows the signal intensity of IFITM1 in 41 HNSCC and 13 normal tissues in microarray analysis in normal and HNSCC tissues. The average of signal intensity of IFITM1 is shown at the bottom of the graph.

Fig. 2. IFITM1 promotes the invasion of HNSCC cells. (**A**) Generation of IFITM1 overexpressing cells. Ca9-22 cells were engineered to overexpressing IFITM1 by transfection with pBICEP-CMV-2-IFITM1. We obtained 3 stable clones of IFITM1 overexpressing cells. Ectopic expression of IFITM1 was examined by immunobloting with anti-FLAG antibody. The whole lysates from all samples were blotted with Cul1 for a loading control. (**B**) Cell proliferation of IFITM1 overexpressing HNSCC cells. Cells were plated on 24 well plates, and trypsinized cells were counted by Cell Counter at 0 and 4 day. We defined 1 as a number of cells at 0 day and calculated the fold change of number of cells at 4 day. (**C**) Invasion of IFITM1 overexpressing HNSCC cells. The invasiveness of the cells was determined by *in vitro* invasion assay. 1.5 x 10^5 cells were placed in the

upper compartment of the cell culture insert for 24 h. To examine the invasiveness, penetrated cells onto the lower side of the filter were fixed with formalin and stained with hematoxylin. We assayed 3 times. (**D**) Migration of IFITM1 overexpressing HNSCC cells. We used one of stable clones for wound healing assay. Migration of the cells was determined by wound healing assay. At 24h after scratching the cells, phase-contrast images (10x field) of the wound healing process were photographed digitally with an inverted microscope. The distance of the wound areas were measured on the images, set at 100% for 0 h, and the mean percentage of the total distances of the wound areas was calculated.

Fig. 3. IFITM1 shRNA inhibited the invasion of HNSCC cells. (**A**) Three different IFITM1 shRNAs were stably transfected in HSC2 cells. After transfection, we treated blastidin for selection. IFITM1 mRNA expression is examined by RT-PCR. GAPDH expression was used as a loading control. (**B**) Cell proliferation of IFITM1 shRNA transfected cells. Cells were plated on 24 well plates and trypsinized cells were counted by Cell Counter at 0 and 4 day. We defined 1 as a number of cells at 0 day and calculated the fold change of number of cells at 4 day. (**C**) Invasion of IFITM1 shRNA transfected cells. The invasiveness of the cells was determined by *in vitro* invasion assay. 1.5×10^5 cells were placed in the upper compartment of the cell culture insert for 24 h. To examine the invasiveness, penetrated cells onto the lower side of the filter were fixed with formalin and stained with hematoxylin. We assayed 3 times.

Fig. 4. Correlation between IFITM1 and CD81 in HNSCC cells. (**A**) Expression of CD81 mRNA in 6 HNSCC cell lines, normal oral epithelial cells and gingival fibroblasts. Expression of CD81 mRNA was performed by RT-PCR. The picture of IFITM1 and

GAPDH mRNA expression is same as Figure 1b. (**B**) CD81 expression was examined in IFITM1 overexpressing and IFITM1 knockdown cells by RT-PCR. The picture of IFITM1 and GAPDH expression in IFITM1 overexpressing and IFITM1 knockdown cells is same as Figure 2a and 3a, respectively. CD81 expression in stable clones of IFITM1 overexpressing cells is shown in upper panel and CD81 expression in IFITM1 shRNAs treated cells is shown in lower panel.

Fig. 5. CD81 is involved in the invasion of HNSCC cells. (**A**) Three different CD81 shRNAs were stably transfected in HSC2 cells. After transfection, we treated blasticidin for selection. CD81 and IFITM1 mRNA expression is examined by RT-PCR. GAPDH expression was used as a loading control. (**B**) Cell proliferation of CD81 shRNA treated cells (upper panel). Cells were plated on 24 well plates and trypsinized cells were counted by Cell Counter at 0 and 4 day. We defined 1 as a number of cells at 0 day and calculated the fold change of number of cells at 4 day. Invasion of CD81 shRNA treated cells (lower panel). The invasiveness of the cells was determined by *in vitro* invasion assay. 1.5 x 10^5 cells were placed in the upper compartment of the cell culture insert for 24 h. To examine the invasiveness, penetrated cells onto the lower side of the filter were fixed with formalin and stained with hematoxylin. We assayed 3 times. (**C**) We examined the co-transfection of CD81 shRNA into IFITM1 transfected HNSCC cells. Three different CD81 shRNAs (#1, 2 and 3) were transiently transfected into IFITM1 overexpressing Ca9-22 cells. IFITM1 and CD81 expression was examined by RT-PCR (upper panel). GAPDH was used as a control. The invasiveness of the cells was determined by *in vitro* invasion assay (lower panel). 1.5 x 10^5 cells were placed in the upper compartment of the cell culture insert for 36 h. To examine the invasiveness, penetrated cells onto the lower side of the filter were fixed with formalin and stained with

hematoxylin. We assayed 3 times. (**D**) IFITM1 is not induced by Wnt/ß-catenin signaling pathway. We treated ß-Trcp1/2 siRNA in HNSCC cells. A 21 nt duplex corresponding to a non-relevant Fbp gene was used as a control. ß-Trcp1/2 siRNA induced down-regulation of ß-Trcp1 and ß-Trcp2 mRNA and accumulation of ß-catenin protein. In this ß-Trcp1/2 siRNA treated cells, IFITM1 mRNA was examined by RT-PCR. GAPDH was used as a control for RT-PCR. Cul1 was used as a loading control for Western blot analysis. (**E**) Gene expression profiles of control and IFITM1 overexpressing HNSCC cells. ZNF236, MMP13 and MMP12 were up-regulated in IFITM1 overexpressing cells (Table 1). We confirmed the expression of ZNF236, MMP13 and MMP12 mRNA in IFITM1 HNSCC overexpressing cells by RT-PCR. GAPDH expression was used as a loading control.

A. Oligonucleotide primer sequences utilized in the RT-PCR

RT-PCR primer set		Sequence	Product length (bp)
IFITM1	F	5'-atgtcgtctggtccctgttc-3'	300
	R	5'-gtcatgaggatgcccagaat-3'	
CD81	F	5'-agatcgccaaggatgtgaag-3'	213
	R	5'-cctccttgaagaggttgctg-3'	
GAPDH	F	5'-tccaccaccctgttgctgta-3'	450
	R	5'-accacagtccatgccatcac-3'	
ßTrcp-1	F	5'-aacggaaactctcagcaagc-3'	240
	R	5'-tggcatccaggtatgacaga-3'	
ßTrcp-2	F	5'-aaaccagcctggaatgtttg-3'	197
	R	5'-cagtccattgctgaagcgta-3'	
ZNF236	F	5'-agctcactcaaaggcggtaa-3'	201
	R	5'-tatagtcctgtcggggttcg-3'	
MMP13	F	5'-ttgagctggactcattgtcg-3'	171
	R	5'-ggagcctctcagtcatggag-3'	
MMP12	F	5'-acacatttcgcctctctgct-3'	192
	R	5'-ccttcagccagaagaacctg-3'	

B. Oligonucleotide sequences utilized for siRNA

shIFITM1		
#1	F	5'-TGCTGTTCAGTTTCTCAGAAGTGTGTGTTTTGGCCACTGACTGACACACACTTGAGAAACTGAA-3'
	R	5'-CCTGTTCAGTTTCTCAAGTGTGTGTCAGTCAGTGGCCAAAACACACACTTCTGAGAAACTGAAC-3'
#2	F	5'-TGCTGACCAGTGACAGGATGAATCCAGTTTTGGCCACTGACTGACTGGATTCACTGTCACTGGT-3'
	R	5'-CCTGACCAGTGACAGTGAATCCAGTCAGTCAGTGGCCAAAACTGGATTCATCCTGTCACTGGTC-3'
#3	R	5'-TGCTGTAATATGGTAGACTGTCACAGGTTTTGGCCACTGACTGACCTGTGACACTACCATATTA-3'
	R	5'-CCTGTAATATGGTAGTGTCACAGGTCAGTCAGTGGCCAAAACCTGTGACAGTCTACCATATTAC-3'
shCD81		
#1	F	5'-TGCTGAGATACAGGAGGTTGGTGGTCGTTTTGGCCACTGACTGACGACCACCACTCCTGTATCT-3'
	R	5'-CCTGAGATACAGGAGTGGTGGTCGTCAGTCAGTGGCCAAAACGACCACCAACCTCCTGTATCTC-3'
#2	F	5'-TGCTGCATACACGCCACCTACATGTGGTTTTGGCCACTGACTGACCACATGTATGGCGTGTATG-3'
	R	5'-CCTGCATACACGCCATACATGTGGTCAGTCAGTGGCCAAAACCACATGTAGGTGGCGTGTATGC-3'
#3	R	5'-TGCTGTTGTGATTACAGTTGAAGGCGGTTTTGGCCACTGACTGACCGCCTTCATGTAATCACAA-3'
	R	5'-CCTGTTGTGATTACATGAAGGCGGTCAGTCAGTGGCCAAAACCGCCTTCAACTGTAATCACAAC-3'

Table 2. List of genes up-regulated by IFITM1 (over 6-fold) in Ca9-22 cells

Ratio(IFITM 1/Control)	Control Normalized	IFITM1 Normalized	Genbank	Common	Description
65.7	0.052373156	3.438695	AK000847	ZNF236	Zinc finger protein 236
23.5	0.040916532	0.95997965	AA053711	EDIL3	EGF-like repeats and discoidin I-like domains 3
19.1	0.29541734	5.6548567	NM_002427	MMP13	Matrix metallopeptidase 13 (collagenase 3)
19.1	0.02700491	0.5164415	AI681013	PRDM2	PR domain containing 2, with ZNF domain
12.5	0.039279867	0.490441	NM_024722	ACBD4	Acyl-Coenzyme A binding domain containing 4
10.1	0.049918167	0.50318635	U50748	LEPR	Leptin receptor
9.6	0.06628478	0.6377772	D49958	GPM6A	Glycoprotein M6A
8.7	0.06382978	0.556207	AF230398	TRIM23	Tripartite motif-containing 23
8.2	0.18903437	1.5421872	NM_002426	MMP12	Matrix metallopeptidase 12 (macrophage elastase)
7.5	0.063011445	0.47004843	AK026191	DDAH2	Dimethylarginine dimethylaminohydrolase 2
7.3	0.7765958	5.682895	NM_005410	SEPP1	Selenoprotein P, plasma, 1
7.0	0.106382966	0.7427989	NM_004585	RARRES3	Retinoic acid receptor responder (tazarotene induced) 3
6.9	0.06873976	0.47667605	AF196478	ANXA10	Annexin A10
6.8	0.2119476	1.4453225	AF096296	CCL26	Chemokine (C-C motif) ligand 26
6.6	0.08428806	0.55365795	AL034410	PCNAP	proliferating cell nuclear antigen pseudogene
6.6	0.091653034	0.60056084	BF939489	GPM6A	Glycoprotein M6A
6.5	0.117839605	0.7687994	AV747166	PARP11	Poly (ADP-ribose) polymerase family, member 11
6.3	0.29214403	1.8307419	AL541302	SERPINE2	Serpin peptidase inhibitor, clade E (nexin, plasminogen activator inhibitor type 1), member 2
6.0	0.07774141	0.46902883	AL037998		CDNA FLJ30740 fis, clone FEBRA2000319

Figure 1

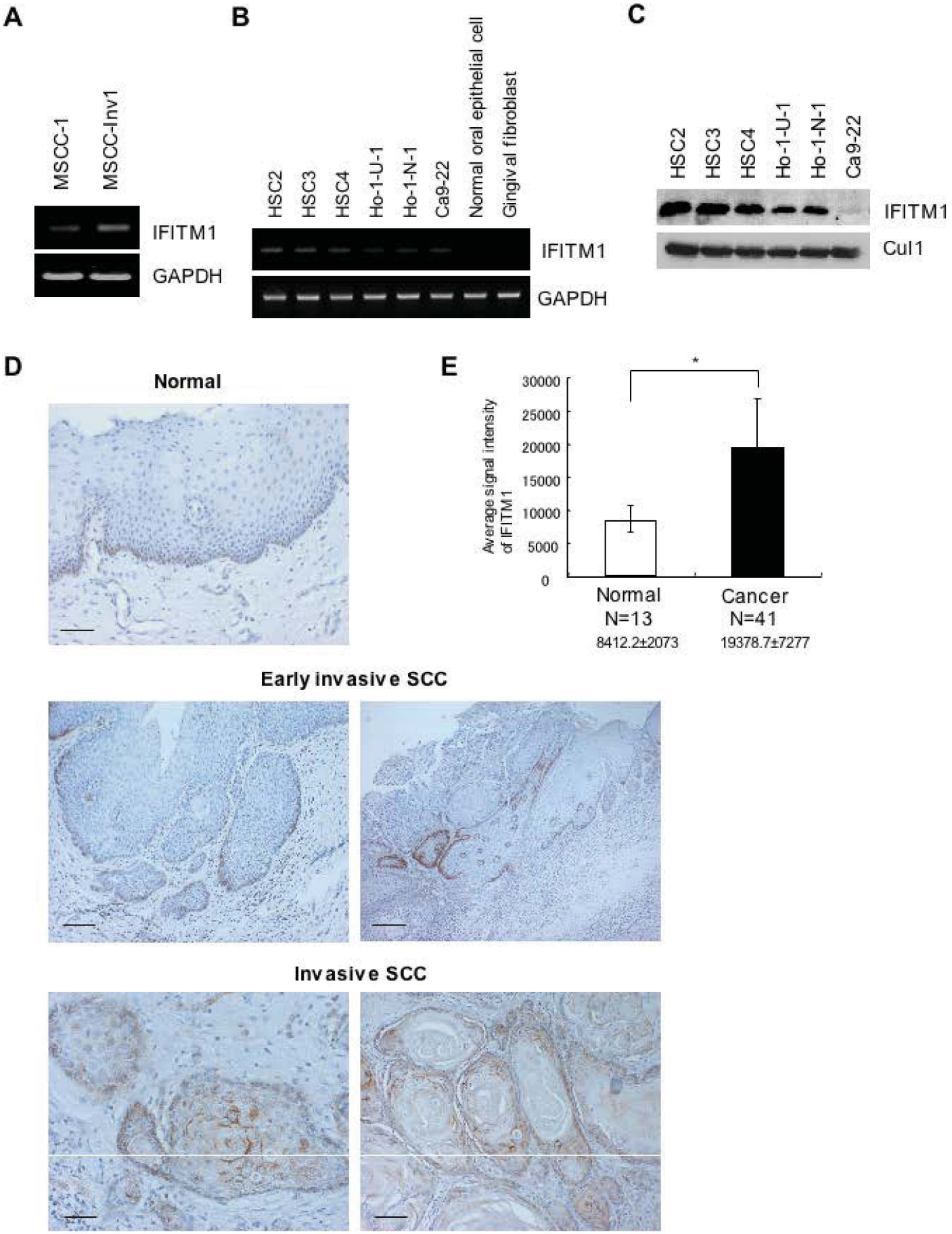
A
MSCC-1
MSCC-Inv1
IFITM1
GAPDH
B
HSC2
HSC3
HSC4
Ho-1-U-1
Ho-1-N-1
Ca9-22
Normal oral epithelial cell
Gingival fibroblast
IFITM1
GAPDH
C
HSC2
HSC3
HSC4
Ho-1-U-1
Ho-1-N-1
Ca9-22
IFITM1
Cul1
D
Normal
Early invasive SCC
Invasive SCC
E
Average signal intensity of IFITM1
30000
25000
20000
15000
10000
5000
0
*
Normal
N=13
8412.2±2073
Cancer
N=41
19378.7±7277

Figure 2

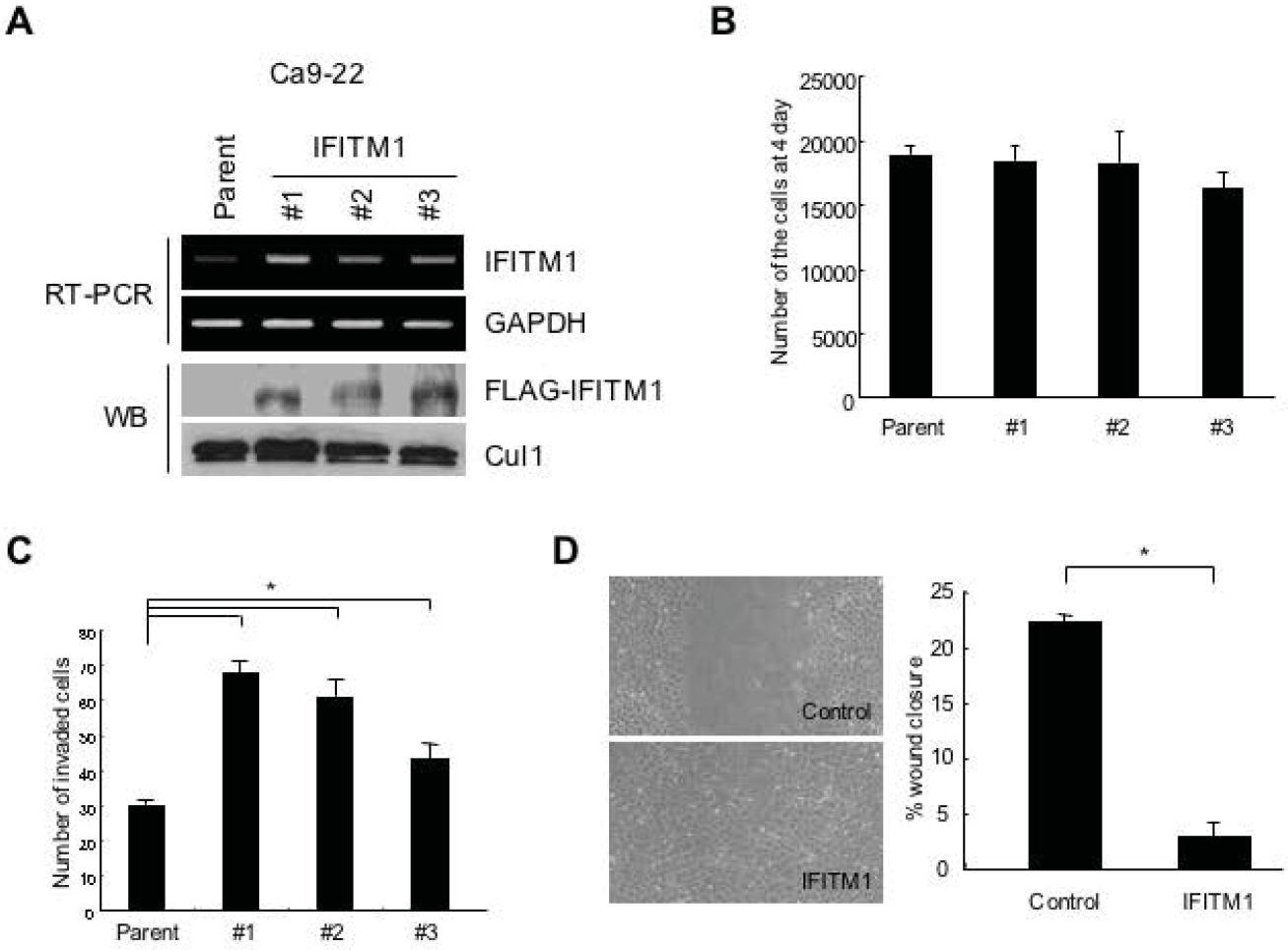
A
Ca9-22
Parent
IFITM1
#1
#2
#3
RT-PCR
IFITM1
GAPDH
WB
FLAG-IFITM1
Cul1
B
Number of the cells at 4 day
25000
20000
15000
10000
5000
0
Parent
#1
#2
#3
C
Number of invaded cells
80
70
60
50
40
30
20
10
0
*
Parent
#1
#2
#3
D
Control
IFITM1
% wound closure
25
20
15
10
5
0
*
Control
IFITM1

Figure 3

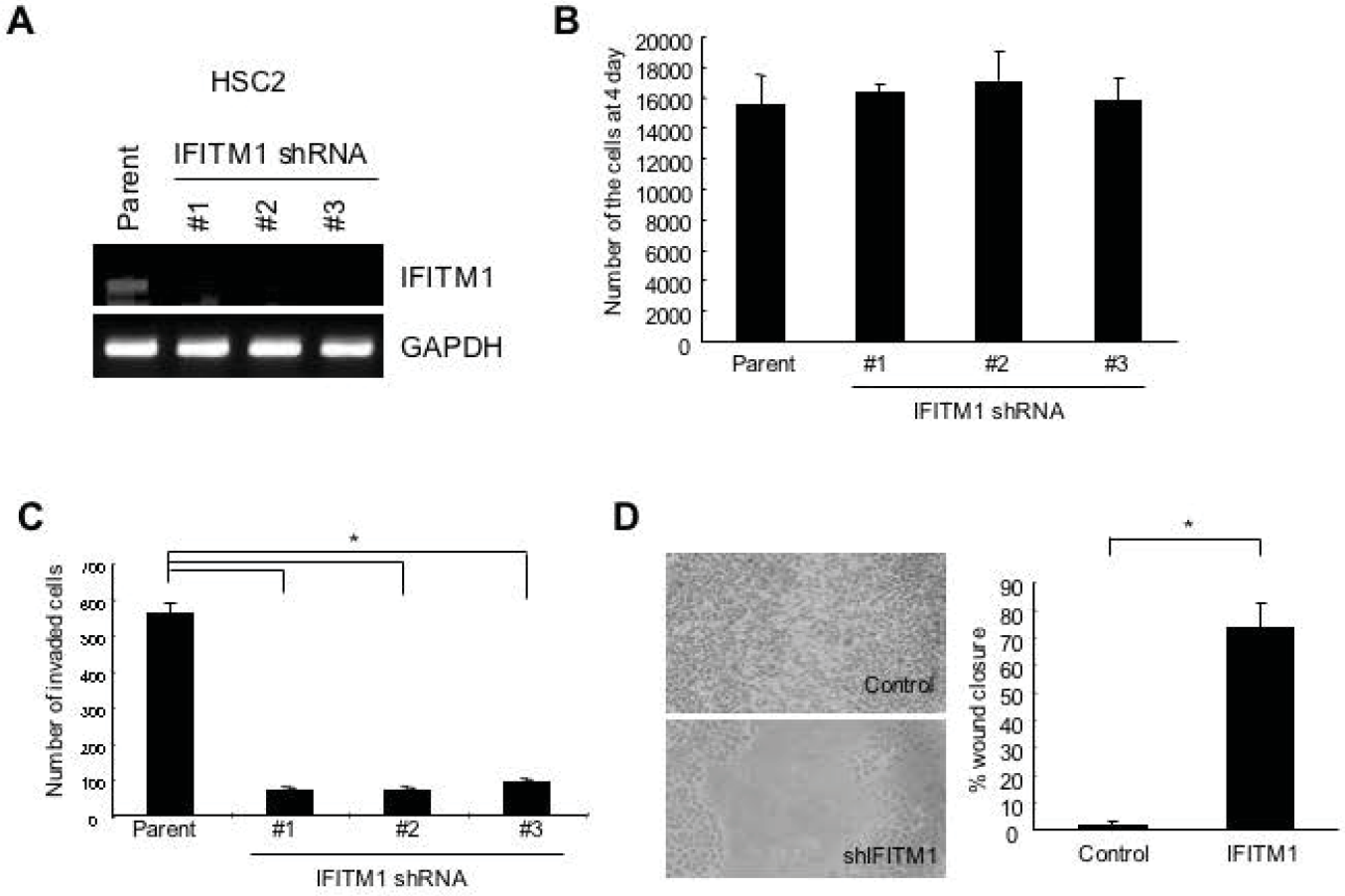
A
HSC2
Parent
IFITM1 shRNA
#1
#2
#3
IFITM1
GAPDH
B
Number of the cells at 4 day
20000
18000
16000
14000
12000
10000
8000
6000
4000
2000
0
Parent
#1
#2
#3
IFITM1 shRNA
C
Number of invaded cells
*
Parent
#1
#2
#3
IFITM1 shRNA
D
Control
shIFITM1
% wound closure
*
Control
IFITM1

Figure 4

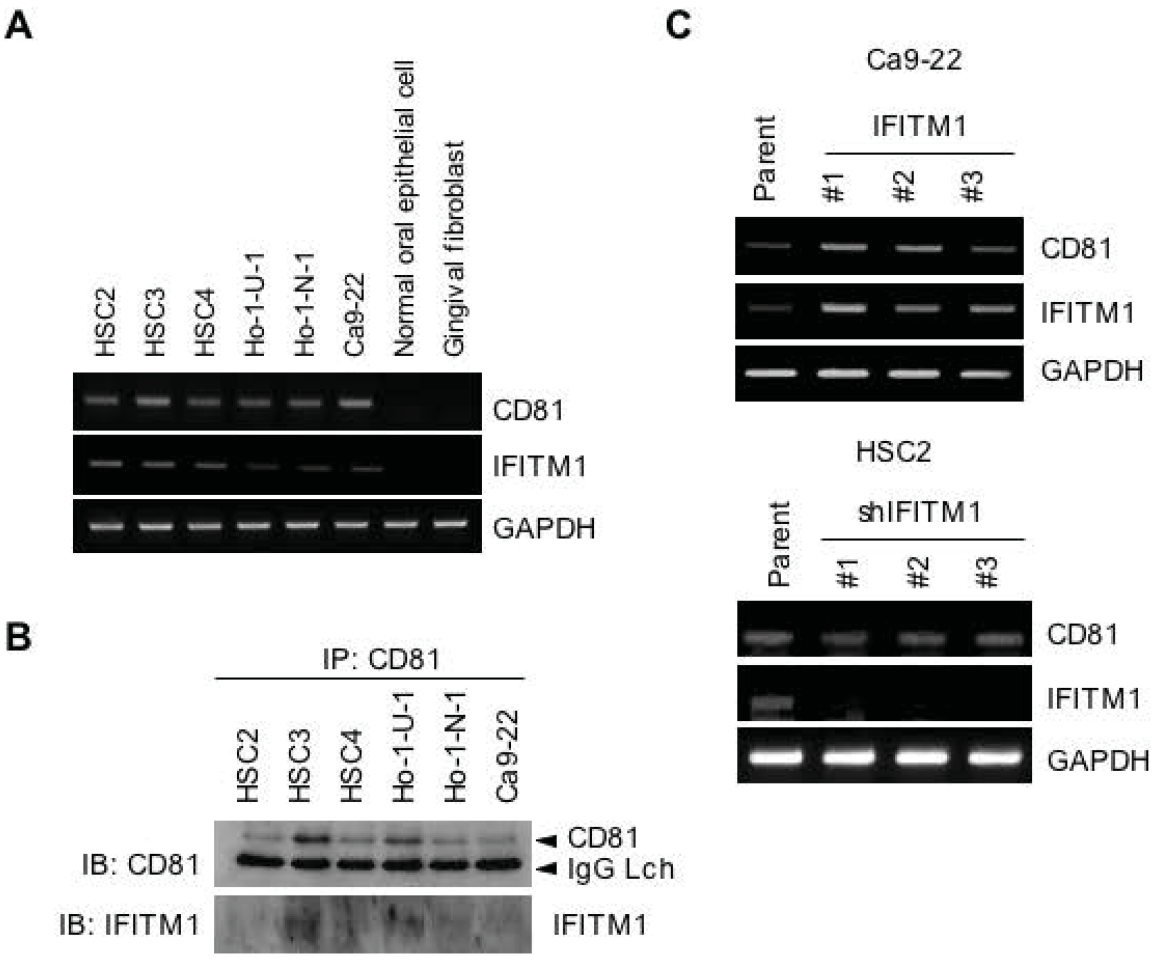
A
HSC2
HSC3
HSC4
Ho-1-U-1
Ho-1-N-1
Ca9-22
Normal oral epithelial cell
Gingival fibroblast
CD81
IFITM1
GAPDH
B
IP: CD81
HSC2
HSC3
HSC4
Ho-1-U-1
Ho-1-N-1
Ca9-22
IB: CD81
CD81
IgG Lch
IB: IFITM1
IFITM1
C
Ca9-22
Parent
IFITM1
#1
#2
#3
CD81
IFITM1
GAPDH
HSC2
Parent
shIFITM1
#1
#2
#3
CD81
IFITM1
GAPDH

Figure 5

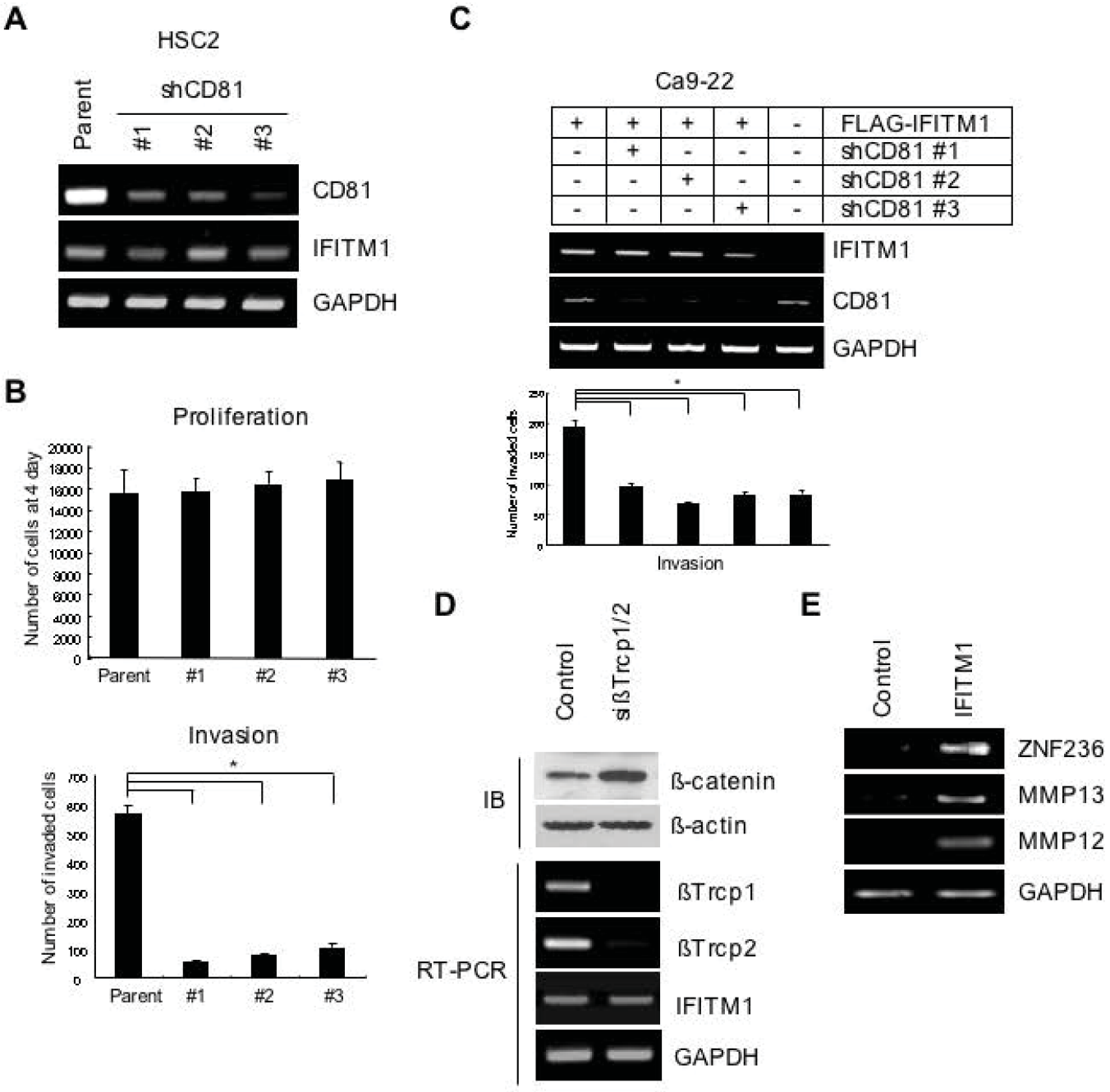
A
HSC2
Parent
shCD81
#1
#2
#3
CD81
IFITM1
GAPDH
B
Proliferation
Number of cells at 4 day
Parent
#1
#2
#3
Invasion
Number of invaded cells
C
Ca9-22
FLAG-IFITM1
shCD81 #1
shCD81 #2
shCD81 #3
IFITM1
CD81
GAPDH
Invasion
D
Control
siβTrcp1/2
IB
ß-catenin
ß-actin
RT-PCR
βTrcp1
βTrcp2
IFITM1
GAPDH
E
Control
IFITM1
ZNF236
MMP13
MMP12
GAPDH